HHS Public Access

Author manuscript

Dev Biol. Author manuscript; available in PMC 2022 May 01.

Published in final edited form as:

Dev Biol. 2021 May ; 473: 33–49. doi:10.1016/j.ydbio.2021.01.012.

Inactivation of Lats1 And Lats2 Highlights the Role of Hippo Pathway Effector YAP in Larynx and Vocal Fold Epithelium Morphogenesis

Vidisha Mohad, PhD[*],
Department of Surgery, University of Wisconsin-Madison, 5118 WIMR, 1111 Highland Avenue, Madison, WI 53705

Vlasta Lungova, PhD[*],
Department of Surgery, University of Wisconsin-Madison, 5105 WIMR, 1111 Highland Avenue, Madison, WI 53705

Jamie Verherden, PhD,
Department of Pediatrics, University of California San Diego, 9500 Gilman Drive, CMME Rm 1087D, La Jolla, CA 92093

Susan L. Thibeault, PhD [Professor]
Department of Surgery, University of Wisconsin School of Medicine and Public Health, 5103 WIMR, 1111 Highland Avenue, Madison, WI 53705

Abstract

Proliferation and differentiation of vocal fold epithelial cells during embryonic development is poorly understood. We examined the role of Hippo signaling, a vital pathway known for regulating organ size, in murine laryngeal development. Conditional inactivation of the Hippo kinase genes Lats1 and Lats2, specifically in vocal fold epithelial cells, resulted in severe morphogenetic defects. Deletion of Lats1 and Lats2 caused abnormalities in epithelial differentiation, epithelial lamina separation, cellular adhesion, basement membrane organization with secondary failed cartilage, and laryngeal muscle development. Further, Lats1 and Lats2 inactivation led to failure in differentiation of p63+ basal progenitors. Our results reveal novel roles of Hippo-Lats-YAP signaling in proper regulation of VF epithelial fate and larynx morphogenesis.

Keywords

Epithelial progenitors; Hippo; YAP; Lat1; Lats2; larynx

corresponding author: Phone: 608-263-0121, thibeaul@surgery.wisc.edu.
[*]Authors contributed equally to the work in this manuscript.

Declaration of interests
The authors have declared that no conflict of interest exists.

Introduction

Voice is generated by specialized tissue, known as vocal folds, housed within the larynx. Millions of individuals throughout the world are affected by voice disorders, due to alterations in vocal fold (VF) mucosa and or tissue loss due to trauma, disease, surgical resection, or nerve dysfunctions, thus impacting VF vibration required for effective phonation [1]. Although the anatomy of VF [2] is well documented, relatively little is known about the embryonic development of the larynx and VF tissue [3–7]. Research focused on cellular and molecular mechanisms of laryngeal embryogenesis is necessary to advance biomedical research efforts utilizing progenitors and stem cells for therapeutic interventions for VF disorders[8, 9,10].

Early stages of laryngeal and VF morphogenesis are closely associated with development of the respiratory diverticulum, which first appears at embryonic (E) day 9.5, in the ventral region of the anterior foregut [11–13]. The most cranial domain of the respiratory diverticulum becomes a part of the primitive laryngopharynx (LPH) that extends cranially to the level of the 4th pharyngeal pouch and gives rise to the prospective larynx and VFs [14,15]. During initial stages of VF embryogenesis, lateral walls of the primitive LPH become closely juxtaposed and temporally fuse to establish the epithelial lamina (EL) at E10.5 and E11.5. The EL is first re-organized to form the tracheoesophageal septum at E13.5 and gradually recanalizes, opening the laryngotracheal tube at E15.5 – E18.5 [16,17]. This is synchronized with the development of the laryngeal cartilages and muscles and stratification of the VF epithelium. The process of EL disintegration is regulated by genes and mechanical forces generated by amniotic fluid passing through the laryngeal inlet down into the lungs [17,18]. Failure in EL recanalization leads to congenital laryngeal webs causing airway obstruction [19,20].

Recently, genes and signaling pathways that control EL formation and recanalization in the larynx have been reported, including Shh and Wnt/beta-Catenin signals that act on proliferation and differentiation of epithelial progenitors and mesenchymal cells [6,7,14]. In the present investigation, we have focused on the Hippo/YAP signaling pathway. In the past decade, YAP (Yes-associated protein), a downstream transcriptional regulator of the Hippo pathway, has emerged as an important manager of cell proliferation, differentiation, apoptosis, and cell fate in development and cancer [21]. The canonical Hippo pathway involves upstream kinases Mst1 and Mst2, which phosphorylate Lats1 and Lats2. Subsequently, Lats1 and Lats2 phosphorylate YAP causing its retention in the cytoplasm and subsequent degradation. When Hippo signaling is disrupted, kinases are inactive, therefore dephosphorylated YAP proceeds to enter the nucleus and interacts with transcriptional enhancer activator domain (TEAD) transcription factor family (homologs of Drosophila Scalloped {Sd}) and other transcription factors to induce expression of genes that are involved in cell proliferation and inhibit apoptosis [21].

In developing lungs, YAP phosphorylation and cytoplasmic localization have been shown to be crucial for the differentiation of epithelial progenitors into distinct cellular phenotypes. YAP is responsible for inducing SOX2 expression, leading to the specification of airway epithelial cell precursors required for lung branching morphogenesis [22]. When

overexpressed, YAP stimulates stem cell proliferation, causing epithelial hyperplasia [22]. YAP overexpression in colonic epithelium causes an expanded progenitor compartment, with a decreased number of differentiated cells[23]. Aberrant nuclear expression of YAP or loss of Mst or Lats kinase activities result in increased liver and heart size due to a surge in cell number [24,25]. Conversely, conditional YAP deletion in the heart causes decreased cardiomyocyte proliferation and lethal embryonic cardiac hypoplasia [26].

As a first step in the interrogation of Hippo/YAP signaling in the developing larynx and VF, we characterized the pattern of YAP and phospho-YAP (p-YAP) expression through VF developmental stages and correlated these expression patterns with major morphogenetic events and cell proliferation. Next, we investigated the function of Lats1 and Lats2, by inactivating these genes in VF epithelium. We demonstrate that throughout laryngeal morphogenesis, both nuclear and cytoplasmic YAP is expressed in proliferating and differentiating VF epithelial progenitors, whereby regulating the normal development of VF epithelium. Conditional deletion of Lats1 and Lats2 in VF epithelial cells leads to nuclear YAP retention which alters epithelial cell proliferation, prevents proper differentiation of basal progenitors and causes severe morphogenetic defects in the VF epithelium and underlying lamina propria. Our data suggest that strict and dynamic control of Hippo-YAP activity is necessary for VF epithelial and laryngeal morphogenesis.

Materials and Methods

Animal Husbandry

All animal studies were carried out with the approval of the University of Wisconsin Madison Institutional Animal Care and Use Committee (IACUC) Protocol M005669. Mice were housed in the Clinical Science Center (CSC), an approved animal facility, and received regular veterinary care and husbandry.

Mouse Models

Developmental and adult expression studies for YAP characterization were performed with wild type FVB/NJ mice. For timed pregnancies, wild type (WT) FVB/NJ males and females were mated. Noon of the day when the vaginal plug of the pregnant female was found was labeled as embryonic day (E) 0.5. Timed pregnant females were sacrificed, and embryos dissected at following embryonic stages: E10.5, E11.5, E13.5, E15.5, E16.5, and E18.5. For postnatal stages, pups were sacrificed, and larynges were dissected at postnatal (P) day: P0, P7, P14, P28, P42 and P56 mice; P42 and P56 are considered adult.

To address the role of Lats1 and Lats2 in the vocal fold epithelium, we conditionally inactivated Lats1 and Lats2 using Shh^{Cre} to create Lats1/2 double mutants using C57BL/6J9 (Black 6) and FVB/NJ mice. $Lats1^{flox}$, $Lats2^{flox}$, and Shh^{cre}; transgenic animal lines have been used previously[27]. First, we bred $Lats1^{flox/flox}$;$Lats2^{flox/flox}$ mice to *Actb-cre* mice (Jackson Laboratory, stock L003376) to generate $Lats1^{D/+}$;$Lats2^{D/+}$ mice. To generate the Lats mutants the Beta-Actin-Cre was used to recombine the Lats Flox allele so that in the double homozygous mutant the Shh-Cre would only have to recombine 2 alleles instead of 4 alleles. The *Actb-cre* is used because it is ubiquitously expressed, making it ideal for

generating null mutants from floxed alleles. The *Actb-cre* is then bred out and the resulting $Lats1^{D/+};Lats2^{D/+}$ mice were then bred to $Shh^{Cre/+}$ mice to create $Lats1^{D/+};Lats2^{D/+};Shh^{Cre/+}$ progeny. Resulting progeny were bred to $Lats1^{flox/flox}$ and $Lats2^{flox/flox}$ to generate epithelial specific knockouts in Lats1 $^{D/flox}$; Lats2$^{D/flox}$; $Shh^{Cre/+}$, resulting in YAP mutants. Lats1 $^{D/flox}$; (Lats2 $^{D/flox}$; $Shh^{Cre/+}$ will be referred to as *Shhcre;Lats* mutant animals). Littermates with the genotype $Lats1^{flox/+}$, $Lats2^{flox/+}$, $Shh^{Cre/+}$ were used as controls. Genotyping of all control and mutant animals was completed using the primer pairs listed in Table 1.

Harvesting and Embedding of Mouse Larynges for Immunofluorescence Staining

All animals were sacrificed following regulations of protocols approved by the University of Wisconsin Animal Care and Use Committee. For embryonic time points, E10.5 through E18.5 whole embryos were dissected from the embryonic cavity, and their neck regions were carefully harvested. For postnatal and adult stages, whole larynges were dissected. Harvested mouse neck regions and larynges were immediately fixed in 4% paraformaldehyde (PFA) in phospho-buffered saline (PBS) at 4°C/overnight, dehydrated in a gradient series of ethanol, treated with xylene, and embedded in paraffin. Paraffin blocks were cut into transverse serial sections (5um) mounted on glass slides and stored in 4°C. For each developmental time-point (12 developmental stages in total), three larynges from three different individuals were dissected and analyzed (n=3; 36 WT larynges in total). In the mutant study, we analyzed three control (n=3) and three mutant (n=3) mice/neck regions at P0 (6 control/mutant larynges in total).

Hematoxylin & Eosin Staining

Paraffin-embedded VF tissue sections were stained with Hematoxylin and Eosin (H&E) using Mayer's hematoxylin (Sigma; MHS16) and Eosin Y alcoholic (Sigma; HT110116) following manufacturer's protocols. Tissue sections were dehydrated by soaking in alcohol and xylene, and placed into a series of chemicals (hematoxylin, acid ethanol, ammonia, and eosin), and mounted in cytoseal. Slides were examined under a Nikon E600 Microscope with Fluorescence equipped with a DP73 camera (Olympus, Center Valley, PA); computer software cellSens (Olympus) was used for image analysis.

Immunofluorescence

Paraffin-embedded VF transverse tissue sections were deparaffinized and rehydrated as noted above followed by antigen retrieval in 10mM citrate buffer pH=6 for 2 hours. Sections were treated with 0.5% triton in PBS for cell membrane permeabilization. Samples were then blocked in 5% bovine serum albumin (BSA) and 5% goat serum in PBS. Primary antibodies used are listed in Table 2. Primary antibodies were applied overnight at 4°C. After washes in PBS + Tween secondary antibodies (Table 3) were applied for 45 min at room temperature (RT). Slides had. a final wash series in PBS + Tween and were stained with DAPI before mounting with Fluromount. Images were taken Nikon E600 Microscope with Fluorescence equipped with an DP73 camera (Olympus); computer software cellSens (Olympus) was used for image analysis.

Immunofluorescence Staining Analysis

Images were taken at various magnification ranging from 10X to 60X, depending upon developmental stage in order to optimize visualization of the laryngeal region to include the thyroid cartilage ventrally and cricoid cartilage dorsally. Images captured were uploaded into ImageJ [28] which was calibrated to provide a scale for all images. Images were taken from similar areas of each slide to maintain consistency. Stained images were qualitatively categorized according to distribution (epithelial vs. mesenchyme), localization (nuclear vs. cytoplasm), and intensity of expression (weak or strong).

Quantification and statistical analysis of proliferation measurements

Proliferation quantification for PH3 assay was done manually using ImageJ. First, for PH3 quantification across twelve developmental time points, the number of PH3 and DAPI-positive cells in the epithelium were counted to determine the percent of proliferating epithelial cells. Means of each group were compared using a General Linear Model procedure with a one-way analysis of variance (ANOVA). To quantitatively evaluate the proliferative activity in control and mutant VF epithelium, the number of PH3 and DAPI positive cells were counted to determine the percentage PH3 positive cells in the VF epithelium. A Student's t-test was used with findings considered statistically significant at $p \leq 0.05$.

Similarly, to quantitatively assess the nuclear/cytoplasmic ratio of YAP in the WT VF epithelium across developmental stages, we manually counted the total number of nuclear and cytoplasmic YAP positive cells in the VF epithelium using Image J. These values were then used to obtain proportions of nuclear to cytoplasmic positive YAP cells and average ratio for each group was graphed in Excel, with ratios as the independent variable and stages of development as the dependent variable. Means of each group were compared using a General Linear Model procedure with a one-way analysis of variance (ANOVA). All findings were considered statistically significant at $p \leq 0.05$.The same procedure was performed in control versus mutant VF epithelium. We manually counted the total number of nuclear and cytoplasmic YAP positive cells in the control and mutant VF epithelium using Image J. These values were then used to obtain proportions of nuclear to cytoplasmic positive YAP cells and average ratio for each group was graphed in Excel, with ratios as the independent variable and control and mutant groups as the dependent variable. A Student's t-test was used findings considered statistically significant at $p \leq 0.05$.

Results

YAP is expressed in VF epithelial cells and its expression changes throughout development

In order to establish a comprehensive baseline of YAP expression and document subsequent intracellular changes, we examined localization of YAP and p-YAP at key developmental stages based on known laryngeal morphogenetic events. First, we assessed the morphology of the developing VF at embryonic and adult stages (Fig. 1). At E10.5 lateral walls of the primitive LPH approach each other at the midline (Fig. 1A) and fuse together and form the epithelial lamina at E11.5 (Fig. 1B). At E13.5, the EL is re-organized to form the

laryngotracheal septum (SPT) (Fig. 1C) and gradually disintegrates (Fig. 1D) to an open airway at E16.5 (Fig. 1E). In the adult stage, VF are separated (Fig. 1F).

Next, we focused on the characterization of the expression pattern of YAP and p-YAP throughout the VF embryonic and postnatal stages, which showed a distinct expression of YAP and p-YAP signals in VF epithelial cells. Intracellular localization of YAP in epithelial cells fluctuated over time and YAP staining was enriched in epithelial cells, when compared to the adjacent mesenchyme. Morphology of VF epithelial cells was highlighted using cytokeratin (K) 8 and 5 (Figs. 2 and 3). In line with our previous investigations [6,16], K8 is strongly expressed in VF epithelial cells during early embryonic stages at E10.5 – 11.5. At E15.5, when VF epithelial progenitors initiate stratification, K8 becomes primarily expressed in the apical cell layer until around birth and it almost disappears from apical layers in postnatal stages and adulthood (Fig. 2). On the other hand, consistent strong K5 expression is detected in VF epithelial cells around the birth and postnatal stages (Figs. 2 and 3). These data show that K8 and K5 can be used as markers of VF epithelial cells at different stages of VF development to assess YAP and p-YAP expression in the VF epithelium.

YAP expression in embryonic stages E10.5 through E18.5

YAP is identified in VF epithelial progenitors as early as E10.5. At this stage, VF epithelium is present in the form of a single layer of columnar epithelial progenitors in the laryngopharyngeal region. We confirmed localization of nuclear YAP, cytoplasmic YAP, and cytoplasmic p-YAP. K8 positive (Fig. 2A) pseudostratified columnar VF epithelial progenitors in the laryngopharyngeal region of the developing larynx at E10.5 shows a precise distribution of nuclear as well as cytoplasmic YAP (Fig. 2B) and weak cytoplasmic p-YAP (Fig. 2C). Epithelial progenitors expressing nuclear YAP, as well as cytoplasmic YAP, can be appreciated in the co-stained images of YAP and p-YAP (Fig. 2D). YAP antibody labels total (nuclear and cytoplasmic form) YAP; hence, cytoplasmic staining along with nuclear localization of YAP in epithelial progenitors is noted. In contrast, p-YAP is weak and unambiguously localized in VF epithelial cell cytoplasm due to the specific binding to the phosphorylated form of YAP.

At E11.5 (Fig. 2E–H), the VF epithelial lamina (EL) which is composed of a single layer of epithelial progenitors show nuclear YAP staining correlating with K8 positive (Fig. 2E and F) epithelial progenitors. At E11.5, there is modification in the morphology as well as the organization of the epithelial progenitors in the EL. Epithelial progenitors go through a change in morphology from its original columnar shape at E10.5, to a cuboidal shape at E11.5 [16]. Concomitant to the change in the morphology and cellular arrangement is the change in intracellular YAP localization. As noted above, YAP is expressed in the nucleus of some of the epithelial progenitors of the EL (Fig. 2F), and p-YAP is expressed only in the cytoplasm (Fig. 2G). Nuclear YAP versus cytoplasmic p-YAP is seen in co-stained sections (Fig. 2H). Weak YAP/p-YAP staining is detected in the mesenchyme of the developing VF at E11.5.

At E13.5, VF epithelial progenitors initiate stratification to form the basal and luminal apical layers of the prospective epithelium. These changes in epithelial organization are

accompanied with YAP expression. YAP is seen both in the nucleus and cytoplasm of the K8 positive cells in the EL (Fig. 2I–L). Between E15.5 and 18.5, the developing VF undergo recanalization, which is associated with VF tissue deformation and VF epithelial remodeling[5]. We detected nuclear as well as cytoplasmic YAP in the VF epithelium at E15.5, (Fig. 2M–P) and mainly E16.5 (Fig. 2Q–T), when the EL recanalization terminates. At E15.5 and E16.5, cytoplasmic YAP correlates with phosphorylation of YAP (Fig. 2 O,S), which is strongly detected in the VF epithelium.

At E18.5, K5 positive epithelial cells (Fig. 2U) continue to express predominantly cytoplasmic YAP(Fig. 2V); only a few nuclear YAP positive cells were detected in the VF epithelium. However, the overall intensity of YAP appears weaker compared to the earlier developmental time points. Localization of p-YAP is seen in Figure 2 (Fig. 2W,X). In VF epithelial cells, the number of positive nuclear YAP cells were greatest between E10.5 and E11.5, whereas cells predominantly expressed cytoplasmic YAP between E13.5 through E18.5 (Fig. 5B). This high nuclear YAP expression at the early stages of the VF and larynx morphogenesis can be associated with increased cell proliferation (Fig. 5). Notably, we also observed an increase in nuclear YAP expression at E16.5 which may be related to VF recanalization and epithelial remodeling.

YAP expression in postnatal stages P0 through P56 (Adult)

In postnatal stages, the laryngeal cavity further develops, as well as the VF epithelium continues to mature from a multi-layered structure in P0 to a multilayered structure in the adult stage. At P0, K5 positive epithelium (Fig. 3A) is three – four layers thick, expressing nuclear and cytoplasmic YAP (Fig. 3B), co-localizing with p-YAP (Fig. 3C, D). Nuclear YAP is localized in the apical compartments. At P7, cytoplasmic YAP continues its expression in K5 positive epithelial cells (Fig. 3E–H) where YAP is co-localized in the cytoplasm with p-YAP. Only a few nuclear YAP positive cells were detected in the apical cell layers (Fig. 3F, H).

At P14 and P28, in the K5 positive epithelial layers (Fig. 3 I, M), VF epithelium further stratifies. In this stratified epithelium, YAP is expressed differently between cells (Fig.3J–P). While nuclear YAP seems to be present primarily in the basal cellular compartment (Fig. 3 J,L,N,P), colocalization of p-YAP (Fig. 3K,O) and cytoplasmic YAP (Fig. 3P,L) is seen more luminally. This change in YAP localization during the postnatal period may indicate a role in epithelial cell stratification.

In the K5 positive adult VF epithelium (Fig. 3Q,U) YAP’s distribution is comparable to what we observed in the later stages of embryonic development. In the adult cells P42 (Fig. 3R–T) and P56 (Fig. 3V–X) VF, nuclear expression of YAP is detected in a few cells only, and the YAP signal has become cytoplasmic. The main difference in YAP expression in the postnatal stages as opposed to the embryonic stages is lower intensity of YAP staining in adult stages versus embryonic. p-YAP expression at P42 and P56 is cytoplasmic. VF epithelial cells predominantly expressed cytoplasmic YAP between P0 through P56.

Distinct nuclear YAP localization in the VF epithelial progenitors correlates with proliferation

To explore the relationship between nuclear YAP and proliferation, we stained for PH3, a marker specific for proliferation (Fig. 4). We detected increased cell proliferation at early embryonic stages E10.5 (Fig. 4A), E11.5 (Fig. 4B) and E13.5(Fig. 4C). At E15.5, PH3 expression declined (Fig. 4D), with increased expression at E16.5 (Fig. 4E). and a decrease again at E18.5 (Fig. 4F). Only a few proliferating cells were detected in the VF epithelium in postnatal stages (Fig. 4G–L). To quantitatively evaluate the percentage of PH3 epithelial cells, we manually counted the number of PH3 positive cells and DAPI positive cells in the VF epithelium across developmental time points. Means and standard deviations for the percent ratios of PH3 and total number of cells in the VF epithelium for the developmental stages examined are seen in Figure 5 (Fig. 5A). A one-way ANOVA between groups showed that there is a significant difference in cellular proliferation across time points ($p < 0.0001$). Proliferation is higher during early developmental stages (E10.5 −13.5) and increases at E16.5 during EL recanalization. PH3 expression significantly decreases during postnatal stages suggesting that epithelial cells enter senescence. (Fig. 5B). To assess whether cell proliferation correlates with YAP retention in the nucleus, we quantitatively evaluated the proportion of nuclear/cytoplasmic YAP. We manually counted the total number of nuclear and cytoplasmic YAP positive cells in the control VF epithelium (3 controls, n=3) and mutant VF epithelium (3 mutants, n=3) using Image J. These values were then used to obtain proportions of nuclear to cytoplasmic positive YAP cells and average ratio for each group was graphed in Excel, with ratios as the independent variable and control and mutant groups as the dependent variable (Fig. 5B). A one-way ANOVA between groups showed that there is a significant difference in YAP location across time points ($p < 0.0001$). Our results show that nuclear YAP translocation correlates with PH3 expression mainly at early stages of VF and laryngeal morphogenesis (E10.5 and E11.5) and then at E16.5 during the EL recanalization, when epithelial cells undergo remodeling to re-establish the epithelial barrier. The increased nuclear YAP detection in postnatal stages P14 and P28 is concomitant with VF epithelial stratification.

Conditional deletion of Lats1 and Lats2 results in nuclear localization of YAP in developing vocal fold epithelial progenitors

With the use of Shh^{Cre}, we inactivated Lats1 and Lats2 in the developing VF epithelium, thus allowing investigation into the functional role of YAP in VF epithelial progenitors. To generate the Lats mutants the *Actb-cre* was used to recombine the Lats Flox allele so that in the double homozygous mutant the Shh-Cre would only have to recombine 2 alleles instead of 4 alleles. The *Actb-cre* is used because it is ubiquitously expressed, making it ideal for generating null mutants from floxed alleles. First, $Lats1^{Flox/Flox};Lats2^{Flox/Flox}$ animals were crossed to *Actb-cre*. All progeny with cre were then $Lats1^{D/+};Lats2^{D/+}$. The *Actb-cre* was crossed out and the $Lats1^{D/+};Lats2^{D/+}$ animals were crossed to Shh^{Cre} to generate the $Shh^{Cre/+};Lats1^{D/+};Lats2^{D/+}$ males used for generating double mutants. We have previously shown that Shh^{Cre} is robustly expressed in VF epithelium throughout development and Shh^{Cre} successfully drives recombination events in VF epithelial cells [6]. Here we have utilized the same strategy and conditionally deleted Lats1 and Lats 2 in VF epithelial cells. In contrast to control embryos ($Lats1^{flox/+}$, $Lats2^{flox/+}$, $Shh^{Cre/+}$ mice) that showed no birth

defects (Fig. 6A), all S*hh*$^{Cre/+}$;*Lats1*$^{D/Flox}$;*Lats2*$^{D/Flox}$ mutants (subsequently referred to as Shhcre;Lats mutant) presented with distinctive birth defects in limbs (upper and lower) and tail, along with loose thickened skin appearance (Fig. 6B) and were lethal at birth. Immunostaining analysis at P0 in the littermate control VF, total YAP was detected throughout the cytoplasm of epithelial cells (Fig. 6C). On the other hand, in the Shhcre;Lats mutants, YAP was present in the nucleus and cytoplasm of the epithelial cells (Fig. 6D). In littermate controls and Shhcre;Lats mutants, p-YAP was nearly absent in the epithelial cells (Fig. 6E, F). YAP localized in the nucleus and cytoplasm of the epithelial cells, not seen in the control VF, indicating that the Hippo/YAP pathways was altered in the Shhcre;Lats mutants ($p < 0.0001$). Our data provides evidence that in the developing VF, conditional deletion of Lats1 and Lats2 causes nuclear localization of YAP. Lastly, the inactivation of Lats1 and Lats2 has been shown to result in an unrestrained growth, ultimately affecting the total size of the organ/tissue. However, for the larynx and VF, we did not see an increase in size.

Nuclear localization of YAP through conditional knockout of Lats1 and Lats2 in epithelium leads to severe morphogenetic defects in larynx and vocal folds

Laryngeal morphology in control and mutant animals immediately at birth (P0) was scrutinized. In controls, VF were separated with an apparent lumen; VF muscles were connected to the thyroid cartilage (TC) (ventrally), arytenoid (AC) and cricoid cartilages (CC) (dorsally) (Fig. 7A). Dorsally, the septum separates the larynx from the esophagus (Fig. 6A,B), with the CC located in the septum (Fig. 7A, B)

In Shhcre;Lats mutants overall laryngeal morphology is significantly altered. We observed severe morphological defects of the VF epithelium, laryngeal cartilages, with disorganized and underdeveloped VF musculature. Mutants (Fig. 7C and D) have partially fused VF epithelium causing considerable occlusion of the glottis unlike the control embryos (Fig. 7A). The glottic space is difficult to discern, and it appears to be filled with a disorganized cell mass (Fig. 7C, D). Attempts at recanalization are visible in the ventral region, where the VF epithelium is lined with a single epithelial cell layer (Fig. 7E). Unseparated VF epithelium obstructs more than seventy-five percent of the glottal region (Fig. 7E, F).

Furthermore, we observed defects in laryngeal cartilages and muscles. The TC is not entirely formed and ACs are distorted (Fig. 7C, D). In the dorsal region of the Shhcre;Lats mutants, an incomplete ring of the CC is evident (Fig. 7C, D). Laryngeal muscles are underdeveloped and disorganized and do not attach to cartilages properly (Fig. 7C, D). The esophagus is entirely deformed and is very likely fused due to the overgrown and deformed CC (Fig. 7C, D).

Nuclear YAP disrupts differentiation of VF epithelial progenitors

To investigate whether inactivation of Lats1 and Lats2 deter differentiation of VF epithelial progenitors, we examined the expression of cytokeratin K8 and p63. K8 an established marker of simple epithelial cells and p63 is a nuclear marker of basal progenitors of the VF epithelium [5,6]. In control animals, K8 is uniformly expressed in the apical layer composed of suprabasal cells and as would be expected, K8 expression is not detected in the basal layer

(Fig. 8 A, B) of the developing VF epithelium. In control VF epithelium, basal cells in the two-layered epithelium expressed p63 (Fig. 8 C, D). As expected, no p63 expression was detected in the suprabasal cells (Fig. 8 C, D). In Shhcre;Lats mutant K8 appears to be expressed in all the epithelial cells of the fused VF (Fig. 8E, F). Closer examination of the VF epithelium revealed positive staining in a single layer of K8 positive progenitors lining the partially open VF epithelium ventrally, as well as the multilayered epithelium obstructing the lumen dorsally (Fig. 8E, F). K8 positive progenitors in the epithelial region show a noticeably abnormally increased thickness as compared to the littermate control. Moreover, in the dorsal region, K8 positive progenitors are also present in the mesenchyme (Fig. 8E, F), which is not seen in control P0 VF.

In the Shhcre;Lats mutant mice, cells in the VF epithelium were p63 negative (−) (Fig. 8G, H) compared to P0 control animals whose basal epithelium was lined with p63+ cells (Fig. 8C, D). A complete absence of the p63+ progenitors in the unseparated VF epithelium may indicate that these cells were not able to instigate p63 differentiation as early as E11.5 due to nuclear YAP expression, or these cells failed to maintain the p63 until they reached P0 developmental stage. These results suggest that inactivation of Lats1 and Lats2 inhibits the differentiation of p63+, and K8− basal cell layer. Instead, epithelial cells retain their simple epithelial phenotype and likely undergo uncontrolled cell division resulting in the formation of disorganized cell mass that prevents VF separation.

Nuclear YAP does not promote proliferation in Lats1 and Lat2 deficient VF

To further investigate the cellular mechanisms by which constitutive nuclear YAP regulates VF development, we examined cell death and proliferation. As the epithelium of the Shhcre;Lats mutant VF appeared multilayered, with disorganized cells spreading into the lumen, we sought to determine if there were less apoptotic cells due to failed recanalization thus resulting in fused VF epithelium. We stained for cleaved caspase 3 (CC3) and found a loss of apoptotic cells in the mutant VF epithelium or adjacent LP as compared to the littermate control mice (Fig. 9A, B).

Because proliferation is a hallmark of Hippo pathway inactivation, we measured cell proliferation by immunostaining with a PH3 antibody to detect proliferating cells. On the contrary to our original assumption, we found few PH3 positive cells within the abnormal VF epithelium in the Shhcre;Lats mutants as compared to controls (Fig. 9C–F). To further confirm this, we performed a quantitative analysis of PH3+ cells versus total number of cells found in the VF epithelium and calculated the percentage of PH3 positive cells in control and mutant VF (Fig. 9G). We found a significant decrease in PH3-positive cells the Shhcre;Lats mutants at P0 compared to control mice ($p = 0.002$). We also noticed that in ShhcreLats1/2 mutants, aberrant DAPI+ VF epithelial cells are smaller than DAPI+ VF epithelial cell in controls and they were closely packed in the middle of the non-existing lumen (Fig. 9C, D). In addition to the quantitative assessment of cell proliferation, we also performed a quantitative analysis of the nuclear/cytoplasmic YAP positive cells in the disrupted VF epithelium to see whether the changes in cell proliferation correlate with nuclear YAP translocation (Fig. 9H). In Shhcre Las1/2 mutants, we found a significant increase in nuclear YAP retention in VF epithelial cells as compared to controls which does

not correspond with the decline in cell proliferation in mutant animals. The decrease in cell proliferation may be explained by the accumulation of undifferentiated cells within the VF lumen triggering spatial competition. Spatial restriction inhibits further expansion and cells self-reorganization in terms of nucleus and cellular sizes.

Conditional inactivation of Lats1 and Lats2 impairs cellular adhesion in the developing VF epithelium

Next, to determine the outcome of Lats1/2 on maintaining epithelial integrity [29], polarity 30 and cellular adhesion in VF epithelium [6], we stained for an adherens junction protein, specifically E-cadherin. In control VF, E-cadherin was expressed strongly in all epithelial cells throughout the entire bilayered epithelium at P0 (Fig. 10A). In Shhcre;Lats mutant VF, localization of E-cadherin was significantly altered. E-cadherin expression was strong and random throughout the entire epithelial region (Fig. 10B). On closer examination, E-cadherin expression appeared more circular, encircling the entire cell, with increased localization on the surface facing the basement membrane. These data suggest that cellular adhesion is impaired in VF epithelial cells due to disruptions in E-cadherin expression.

Conditional deletion of Lats1 and Lats2 results in alteration of VF basement membrane components

We further investigated how YAP's presence in epithelial cells alters the structure and organization of the VF basement membrane. We examined expression of Laminin α5 (Lama5) and collagen IV (Col IV) proteins, fundamental constituents of an intact VF basement membrane. In control VF, a fully developed and intact basement membrane was present as confirmed by anti-Lama5 staining (Fig. 10C). Conversely, in Shhcre;Lats mutant VF, the basement was strikingly disjointed and lacked continuity throughout the disorganized epithelium structure. Lama5 appeared broken, with visible disintegration (Fig. 10D), suggesting that the stability of the basement membrane, was compromised.

In control VF at P0, collagen IV expression was intense, and continuous throughout the VF epithelium (Fig. 10E). In control VF, collagen IV expression co-localized with Laminin α5 (Fig. 10C, E). In Shhcre;Lats mutants, collagen IV was expressed; however, the expression was aberrant and disorganized (Fig. 10F). On closer examination, collagen IV fibers appeared to be abnormally double-layered, instead of a single layer (Fig. 10F). Circular rings of collagen IV are noted in numerous regions of the thickened and disorganized VF epithelium. Altogether, these data reveal that Lats1 and Lat2 conditional knockouts have disrupted basement membrane formation.

Aberrant nuclear YAP expression in VF epithelium causes defects in mesenchyme

Major constituents of an intact larynx are primarily cartilages, muscles, and connective tissue [3,6]. Given the mesenchymal defects initially identified on histological staining, we were interested in understanding if aberrant nucleau YAP expression affects the development of mesenchymal structures. We further investigated development of laryngeal cartilages by immunofluorescence staining with SOX9 antibody, which is specific for cartilage, and myosin heavy chain (MF) 20 antibody for emerging laryngeal muscles.

In control VF, SOX9 was detected primarily in the laryngeal cartilages, specifically in cricoid cartilage, along with the C-shaped thyroid and arytenoid cartilages, which are essential for the laryngeal support (Fig. 11A, C). In the control VF, MF-20, expressing cells were detected in the main groups of laryngeal muscles comprised of thyroarytenoid muscle attached to the thyroid lamina (ventrally) (Fig. 11B, C), and dorsal laryngeal muscles connecting the arytenoid cartilages with the cricoid cartilage dorsally (Fig. 11B, C). These muscles were fully developed (Fig. 11B, C).

In the Shhcre;Lats mutants, severe defects in laryngeal cartilages and muscles in the developing mesenchyme (Fig. 11D–I) were noted. In the deformed thyroid cartilage, a very small cluster of cells expressed SOX9, resulting in distorted development of the thyroid lamina. We also noticed a reduced expression of SOX9 in the AC (Fig. 11D,F). Interestingly, SOX9 positive cells were absent in the cricoid cartilage, resulting in malformed CC shape and function (Fig. 11D,F, G). In the Shhcre;Lats mutants, parallel to the abnormalities in the differentiation of laryngeal cartilages, we found significant defects in laryngeal muscle development (Fig. 11E, F). Along with a sharp reduction in SOX9 expression, there was marked disorganization of MF-20 expressing mesenchymal cells, especially in the ventral laryngeal region as compared to littermate controls (Fig. 11H, I). The thyroarytenoid muscle appears shrunken and has significantly reduced muscle mass, as well as its attachment into the thyroid cartilage, was distorted. Similarly, the dorsal laryngeal muscles were visible, however their mass and attachments were distorted too due to the aberrant development of the CC and AC. (Fig. 11H, I). Taken together, these data provide evidence that VF epithelial progenitors interact with the surrounding mesenchyme, thus regulating mesenchymal differentiation during VF morphogenesis. Inactivation of Lats1/2 in the epithelium results in the impaired differentiation of mesenchymal cells in the larynx.

Discussion

Despite the central role of the larynx in mammalian communication, there is a paucity of work related to the development of this tissue with a limited number of publications characterizing its morphogenesis [5–7]. In this study, we have made an effort to fill a fundamental gap in the understanding of the intricately orchestrated morphogenesis of the larynx and VF. The present study provides evidence that Hippo/YAP signaling is involved in regulation of proliferation and differentiation of VF epithelial progenitors. Specifically, deletion of Lats1/2 resulted in the failed separation of epithelial lamina and differentiation of basal p63 epithelial progenitors, loss of epithelial differentiation and cellular adhesion, and impaired basement membrane organization. Inactivation of Lats 1/2 in VF epithelium also contributed to defects in the mesenchymal compartment - failed cartilage and laryngeal muscle development.

Our study demonstrates that the Hippo pathway downstream effectors, YAP and phospho-YAP must be strictly regulated in VF epithelial cells throughout the development. YAP is primarily expressed in VF epithelial cells and its localization fluctuates between the nucleus and cytoplasm through development. In agreement with our hypothesis, YAP is found to be enriched in VF epithelial progenitors compared to the mesenchyme. Nuclear YAP expression is higher in early developmental stages (E10.5 through E11.5), then YAP is

transferred from the nucleus into the cytoplasm and becomes unphosphorylated at E16.5 during the EL recanalization. In more advanced stages of the VF and laryngeal embryogenesis and postnatally, YAP expression is primarily cytoplasmic with a slight increase in nuclear YAP at P14 and P28 during epithelial stratification. Nuclear YAP correlates with major morphogenetic events and cellular processes described previously[5]. First, the murine laryngopharyngeal region at E10.5 is composed of a single layer of pseudo-columnar epithelial progenitors, which convert into a single layer of basal epithelial progenitors that gradually stratify and covert into multilayered structure in adulthood. During morphogenesis, starting at E10.5, some epithelial cells in the laryngeal cavity undergo proliferation as measured by PH3. At this time point, YAP is localized in both the nucleus and cytoplasm of the pseudo-columnar epithelial progenitor's cells. This suggests that YAP is involved in regulation of the cell proliferation that is required for approaching of the lateral walls at the center of the lumen and formation of the EL at E11.5. Beside increased cell proliferation, epithelial cells initiate differentiation into basal progenitors expressing p63, which occurs at E11.5[5,6]. p63, a well-known master switch gene of epithelial stratification[31] is absent in the columnar epithelial cells at E10.5. Our results suggest that nuclear presence of YAP during early stages of laryngeal embryogenesis may be also associated with changes in cellular morphology and basal cell differentiation occurring at E11.5. There are two explanations for the cytoplasmic retention of YAP during basal cell differentiation. First, decline in YAP protein levels in some cells is due to YAP ubiquitination and degradation triggered by Ser381 phosphorylation, and second, due to YAP phosphorylation at S127 [32]. There is an increase in the YAP protein phosphorylation at E11.5, supporting our contention that YAP becomes cytoplasmic during onset of differentiation. Published literature specific to embryonic lung development has demonstrated that YAP nucleocytoplasmic translocation coordinates cellular proliferation and differentiation during the airway epithelial branching, and lung patterning[22,33,34]. Another increase in nuclear unphosphorylated YAP can be seen at E16.5. At this time point EL completes recanalization, VF tissue deforms, and epithelial cells undergo intense remodeling[14]. Nuclear YAP translocation can be therefore associated with proliferation changes in basal epithelial cells as a potential mechanism to maintain the epithelial protective barrier. In the postnatal period, the expression of nuclear YAP in the basal cell layer of the VF epithelium at P14 and P28 is suggestive of a conceivable role in stratification. Strong correlation between nuclear YAP and cycling activity of epidermal stem cells has been reported during epidermal stratification[35]. In mature epidermis, it has been shown that quiescent cytoplasmic YAP becomes nuclear during the growth phase when the basal stem cells are in active stage of cycling[36]. Future studies will explore the role of nuclear YAP in basal cells during VF epithelium stratification.

In the Shhcre;Lats mutants, deletion of the Hippo pathway downstream genes Lats1 and Lats2 in developing VF epithelium led to nonphosphorylated nuclear YAP, resulting in severe morphogenetic defects of the larynx and VF. In Shhcre;Lats mutants there is an increase in K8 positive cells, incomplete separation of VF epithelium, failed basal cell differentiation, impaired cell adhesion, and secondarily deformed musculature and cartilages. In agreement with other studies, the findings from this study demonstrate that with inactivation of Lats1 and Lats2, there is a halt in morphogenesis. Although, no tissue

overgrowth was observed in the Shhcre;Lats mutants, despite nuclear nonphosphorylated YAP, similar severe phenotypes have been reported by other studies [37–40]. The larynx is made from multiple tissue types and is surrounded by muscle and cartilages that might have limited growth or size expansion of this tissue. Lastly, YAP signaling was disrupted in the epithelium with a limited effect on the adjacent mesenchyme, as few Shhcre epithelial cells may delaminate from the EL and incorporate into the lamina propria at early stages of the laryngeal morphogenesis[5]. Severe defects seen in the mesenchymal compartment may, therefore be secondary to defective Hippo-YAP signaling in the VF epithelium. This could explain why an overall increase in the size of the VF was not seen. It is arguable that in Shhcre;Lats mutants, VF tissue appears to be overgrown on morphological examination, however, this could be due the fact that cartilage was absent and there is an enlarged lumen filled with undifferentiated epithelial cells whereby there is distortion in the morphological appearance of this tissue.

To further uncover the origin of the cell mass in the VF lumen of mutant animals, we evaluated the expression levels of PH3 and CC3 to investigate whether this abnormal nuclear YAP retention can cause the increase in cell proliferation and/or inhibit the cell death. We found no apoptotic cells and significantly reduced cell proliferation in the mutant VF epithelium at P0 stage. Although we did not detect intense cell proliferation at P0 stage, it is possible that cells underwent cell division at earlier developmental stages and by P0 entered the senescence due to spatial restrictions.

Besides aberrant cellular processes such as apoptosis and cell proliferation, retention of YAP in the nucleus seems to also impair VF basal cell differentiation and cell adhesion. Shhcre;Lats mutant VF show only a single-layered, not entirely separated VF epithelium with p63-K8+ cells. The large pool of K8 positive cells in the disorganized epithelium of the Shhcre;Lats mutant show pseudostratified columnar phenotype, which is atypical in normal VF epithelium at P0 stage. This disordered p63- K8+ layer suggest that epithelial cells at earlier embryonic time points were unsuccessful in differentiating into basal cells resulting in the simplification of this tissue layer. This is supported by work that has shown enlarged basal cells progenitors populations of p63- K5+ in the trachea of Lats mutants [37]. Another report in the lung presents evidence that nuclear YAP severely impaired proximal-distal epithelium identity and epithelial differentiation [41].

Our finding of disrupted E-cadherin expression in VF epithelium in the Shhcre;Lats mutants is in agreement in other reports in the literature, in the lung and kidney, that describe disrupted E-cadherin expression with YAP overexpression [34,37,42]. This fragmented expression of E-Cadherin, suggests that cell-cell adhesion in the epithelium of the Shhcre;Lats mutant is disrupted. Current evidence in the literature postulates that there is a possible feedback circuit between E-cadherin and Hippo signaling [43]. The feedback between E-cadherin and Hippo pathway [43] likely regulates diverse cellular mechanisms and changes in the microenvironment to allow synchronized morphogenesis of the VF, as seen in the submandibular gland [44]. The defects in differentiation and proliferation observed in Shhcre;Lats mutant VF could be secondary, due to the primary defects in E-cadherin. As cell adhesion regulates critical cellular processes such as proliferation and differentiation, it is

probable that VF epithelial progenitors failed to differentiate and continue to proliferate resulting in increased VF epithelial progenitor population in the mutant VF epithelium.

It is evident that although nuclear YAP is essential in governing critical cellular processes, timely phosphorylation of YAP is equally crucial for proper VF morphogenesis. As evidenced in this study, dynamic Hippo signaling activity during VF morphogenesis goes beyond the simplified view that Hippo pathway disrupts tissue growth by merely increasing cellular proliferation. Collective morphogenetic defects seen in the Shhcre;Lats mutant VF epithelium suggest that the Hippo pathway may be involved in regulating the establishment and differentiation of VF epithelial progenitors, cell adhesion, and basement membrane integrity. Further work is warranted investigating Shh-cre, Lats1/2 mutants at developmental time points prior to P0 to determine timing of Hippo pathway initiation.

Acknowledgments

Funding

This work was funded by the NIH NIDCD R01 DC04336 and DC012773.

References:

1. Friedrich G et al. Vocal fold scars: Current concepts and future directions. Consensus report of the phonosurgery committee of the European laryngological society. Eur. Arch. Oto-Rhino-Laryngology 270, 2491–2507 (2013).
2. Kakodkar KA, Schroeder JW & Holinger LD Laryngeal development and anatomy. in Pediatric Airway Surgery (2012). doi:10.1159/000334108
3. Henick DH Three-dimensional analysis of murine laryngeal development. Ann. Otol. Rhinol. Laryngol. (1993).
4. Hopp ES The development of the epithelium of the larynx. Laryngoscope 65, 475–499 (1955). [PubMed: 13243776]
5. Lungova V, Verheyden JM, Herriges J, Sun X & Thibeault SL Ontogeny of the mouse vocal fold epithelium. Dev. Biol. 399, 263–282 (2015). [PubMed: 25601450]
6. Lungova V, Verheyden JM, Sun X & Thibeault SL β-catenin signaling is essential for mammalian larynx recanalization and the establishment of vocal fold progenitor cells. Dev. 145, (2018).
7. Tabler JM et al. Cilia-mediated hedgehog signaling controls form and function in the mammalian larynx. Elife (2017). doi:10.7554/eLife.19153
8. Jensen JN et al. Recapitulation of elements of embryonic development in adult mouse pancreatic regeneration. Gastroenterology 128, 728–741 (2005). [PubMed: 15765408]
9. Fishman JM et al. Stem cell approaches for vocal fold regeneration. Laryngoscope 1–6 (2016). doi:10.1002/lary.25820
10. Lungova V, Leydon C & Thibeault S Derivation of epithelial cells from human embryonic stem cells as an in vitro model of vocal mucosa. Methods Mol. Biol. 1307, 237–243 (2015).
11. Morrisey EE & Hogan BLM Preparing for the first breath: genetic and cellular mechanisms in lung development. Dev. Cell 18, 8–23 (2010). [PubMed: 20152174]
12. Herriges M & Morrisey EE Lung development: Orchestrating the generation and regeneration of a complex organ. Dev. 141, 502–513 (2014).
13. Zepp JA & Morrisey EE Cellular crosstalk in the development and regeneration of the respiratory system. Nat. Rev. Mol. Cell Biol. 20, 551–566 (2019). [PubMed: 31217577]
14. Lungova V & Thibeault SL Mechanisms of larynx and vocal fold development and pathogenesis. Cell. Mol. Life Sci. (2020). doi:10.1007/s00018-020-03506-x

15. Henick DH Three-Dimensional Analysis Of Murine Laryngeal Development. Ann. Otol. Rhinol. Laryngol. Suppl. 159, 3–24 (1993). [PubMed: 8457128]
16. Lungova V, Verheyden JM, Herriges J, Sun X & Thibeault SL Ontogeny of the mouse vocal fold epithelium. Dev. Biol. 399, (2015).
17. Lungova V, Verheyden JM, Sun X & Thibeault SL β-catenin signaling is essential for mammalian larynx recanalization and the establishment of vocal fold progenitor cells. Dev.145, (2018).
18. Lungova V, V.Griffin K, Lunga T & L.Thibeault S Drainage of amniotic fluid delays vocal fold separation and induces load-related vocal fold mucosa remodeling. Dev. Biol. in press, (2020).
19. Ahmad SM & Soliman AMS Congenital anomalies of the larynx. Otolaryngol. Clin. North Am. 40, 177–91 (2007). [PubMed: 17346567]
20. Liberty G et al. The fetal larynx and pharynx: Structure and development on two- and three-dimensional ultrasound. Ultrasound Obstet. Gynecol. 42, 140–148 (2013). [PubMed: 23239522]
21. Pan D The hippo signaling pathway in development and cancer. Developmental Cell (2010). doi:10.1016/j.devcel.2010.09.011
22. Mahoney JE, Mori M, Szymaniak AD, Varelas X & Cardoso WV The Hippo Pathway Effector YAP Controls Patterning and Differentiation of Airway Epithelial Progenitors. Dev. Cell (2014). doi:10.1016/j.devcel.2014.06.003
23. Camargo FD et al. YAP1 Increases Organ Size and Expands Undifferentiated Progenitor Cells. Curr. Biol. (2007). doi:10.1016/j.cub.2007.10.039
24. Zhou D et al. Mst1 and Mst2 Maintain Hepatocyte Quiescence and Suppress Hepatocellular Carcinoma Development through Inactivation of the YAP1 Oncogene. Cancer Cell 16, 425–438 (2009). [PubMed: 19878874]
25. Heallen et al. Hippo signaling impedes adult heart regeneration. Development 140, 4683–4690 (2013). [PubMed: 24255096]
26. Xin M et al. Regulation of Insulin-Like Growth Factor Signaling by YAP Governs Cardiomyocyte Proliferation and Embryonic Heart Size. Sci. Signal. (2011). doi:10.1126/scisignal.2002278
27. Heallen T et al. Hippo pathway inhibits wnt signaling to restrain cardiomyocyte proliferation and heart size. Science (80-.). (2011). doi:10.1126/science.1199010
28. Schneider CA, Rasband WS & Eliceiri KW NIH Image to ImageJ: 25 years of image analysis. Nat. Methods (2012).
29. Van Roy F & Berx G The cell-cell adhesion molecule E-cadherin. Cellular and Molecular Life Sciences (2008). doi:10.1007/s00018-008-8281-1
30. Desai RA, Gao L, Raghavan S, Liu WF & Chen CS Cell polarity triggered by cell-cell adhesion via E-cadherin. J. Cell Sci. (2009). doi:10.1242/jcs.028183
31. Koster MI, Kim S, Mills AA, Demayo FJ & Roop DR p63 is the molecular switch for initiation of an epithelial stratification program. 14, 126–131 (2004).
32. Zhao B, Li L, Lei Q & Guan K The Hippo – YAP pathway in organ size control and tumorigenesis : an updated version. Cold Spring Harb. Press (2010). doi:10.1101/gad.1909210
33. Lange AW et al. Hippo/YAP signaling controls epithelial progenitor cell proliferation and differentiation in the embryonic and adult lung. J. Mol. Cell Biol. (2015). doi:10.1093/jmcb/mju046
34. Szymaniak AD, Mahoney JE, Cardoso WV & Varelas X Crumbs3-Mediated Polarity Directs Airway Epithelial Cell Fate through the Hippo Pathway Effector YAP. Dev. Cell (2015). doi:10.1016/j.devcel.2015.06.020
35. Elbediwy A, Vincent-Mistiaen ZI, Spencer-Dene B, Stone RK, Boeing S, Wculek SK, Cordero J, Tan EH, Ridgway R, Brunton VG, et al. Integrin signaling regulates YAP and TAZ to control skin homeostasis. Development. 2016;143:1674–1687. doi: 10.1242/dev.133728. [PubMed: 26989177]
36. Beverdam A, Claxton C, Zhang X, James G, Harvey KF, Key B YAP Controls Stem/Progenitor Cell Proliferation in the Mouse Postnatal Epidermis. J. Invest. Derm. 2013;133:1497–1505. doi: 10.1038/jid.2012.430 [PubMed: 23190885]
37. Nantie LB et al. Lats1/2 inactivation reveals Hippo function in alveolar type I cell differentiation during lung transition to air breathing. Development 145, dev163105 (2018). [PubMed: 30305289]

38. Szymaniak AD et al. The Hippo pathway effector YAP is an essential regulator of ductal progenitor patterning in the mouse submandibular gland. Elife (2017). doi:10.7554/elife.23499

39. Chung C et al. Hippo-Foxa2 signaling pathway plays a role in peripheral lung maturation and surfactant homeostasis. Proc. Natl. Acad. Sci. (2013). doi:10.1073/pnas.1220603110

40. Lin C, Yao E & Chuang PT A conserved MST1/2-YAP axis mediates Hippo signaling during lung growth. Dev. Biol. (2015). doi:10.1016/j.ydbio.2015.04.014

41. Van Soldt BJ et al. YAP and its subcellular localization have distinct compartmentspecific roles in the developing lung. Development (2019). doi:10.1242/dev.175810

42. McNeill H & Reginensi A Lats1/2 Regulate YAP/Taz to Control Nephron Progenitor Epithelialization and Inhibit Myofibroblast Formation. J. Am. Soc. Nephrol. (2016). doi:10.1681/asn.2016060611

43. Kim, Koh E, Chen X & Gumbiner BM E-cadherin mediates contact inhibition of proliferation through Hippo signaling-pathway components. Proc. Natl. Acad. Sci. (2011). doi:10.1073/pnas.1103345108

44. Walker JL et al. Diverse roles of E-cadherin in the morphogenesis of the submandibular gland: Insights into the formation of acinar and ductal structures. Dev. Dyn. (2008). doi:10.1002/dvdy.21717

Highlights:

- Hippo signaling governs laryngeal and vocal fold morphogenesis by regulating epithelial progenitor proliferation and differentiation
- Lats1 and Lats2 inactivation led to failure of complete separation of the epithelial lamina
- Lats1 and Lats2 inactivation results in nuclear YAP retention
- Lats1 and Lats2 null vocal fold exhibit altered epithelial cell proliferation and basal progenitor differentiation with severe morphogenetic defects in the epithelium and lamina propria

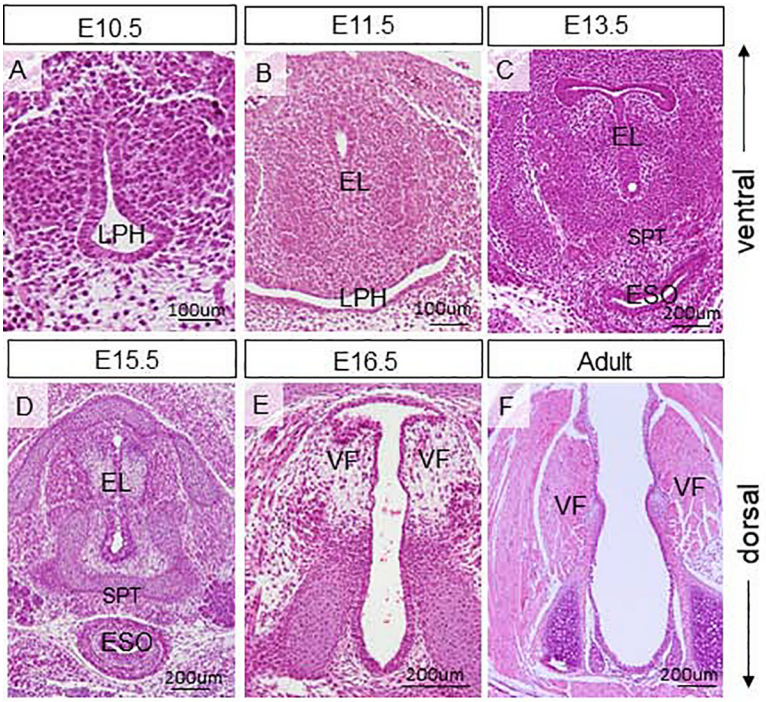

Figure 1: Morphology of the developing vocal folds.

(A-F) Hematoxylin-eosin staining in the vocal fold transversal sections showing the vocal fold morphology at embryonic stages E10.5 (A), E11.5 (B), E13.5 (C), E15.5 (D), E16.5 (E) and adult (F). Abbreviations: EL, epithelial lamina; ESO, esophagus; LPH, primitive laryngopharynx; SPT, septum; VF, vocal folds.

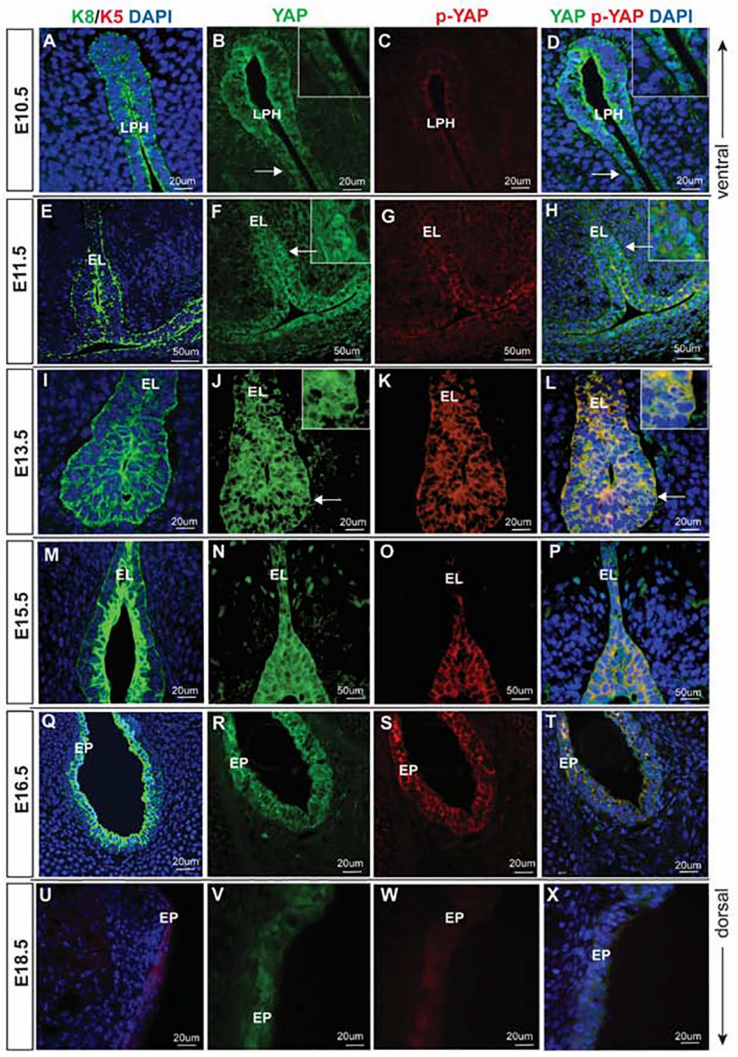

Figure 2: YAP expression in embryonic VF epithelial development.

(A-D) Transverse sections of mouse primitive laryngopharynx at E10.5. IF analysis of K8 (green) (A), total YAP (green) (B), p-YAP (red) (C) and double staining of YAP and p-YAP (yellow) (D). Prominent nuclear YAP in seen in K8 positive progenitors. White solid arrows in the panels of B, D denote nuclear YAP positive cells. These regions are magnified in the same panels in the upper right corners. (E-H) Transverse sections of mouse laryngeal cavity at E11.5. IF analysis of K8 (green) (E), total YAP (green) (F), p-YAP (red) (G) and double staining of YAP and p-YAP (yellow) (H). White solid arrows in the panel of F, H denote nuclear YAP positive cells. These regions are magnified in the same panels in the upper right corners. (I-L) Transverse sections of mouse laryngeal cavity and VF at E13.5. IF analysis of K8 (green) (I), total YAP (green) (J), p-YAP (red) (K) and double staining of YAP and p-YAP (yellow) (L). YAP continuous to be nuclear at this stage and p-YAP is cytoplasmic. White solid arrows in the panels of J, K indicate nuclear YAP positive cells. These regions are magnified in the same panels in the upper right corners. (M-P) Transverse sections of mouse VF at E15.5. IF analysis of K8 (green) (M), total YAP (green) (N), p-YAP (red) (O) and double staining of YAP and p-YAP (yellow) (P). YAP is no longer nuclear in VF

epithelial progenitors at this stage. Nucleocytoplasmic shift in YAP localization occurs at E15.5 resulting in total YAP (green) and p-YAP (red) co-localizing together in the cytoplasm. (Q-T) Transverse sections of mouse VF at E16.5. IF analysis of K8 (green) epithelial marker (Q), total YAP (green) (R), p-YAP (red) (S) and double staining of YAP and p-YAP (yellow) (T). (U-X) Transverse sections of mouse VF at E18.5. K5 (red) (U), total YAP (green) (V), p-YAP (red) (W) and double staining of YAP and p-YAP (yellow) (X). YAP is detected only in the cytoplasm where it co-localizes with the p-YAP. Primary antibodies are color-coded according to their secondary antibodies, and nuclei are counterstained with DAPI. IF images were taken at 40X and 60X magnification. Scale bar of 50um and 20um are denoted in figure panels. Abbreviations: LPH, laryngopharynx; EL, epithelial lamina; EP, epithelium.

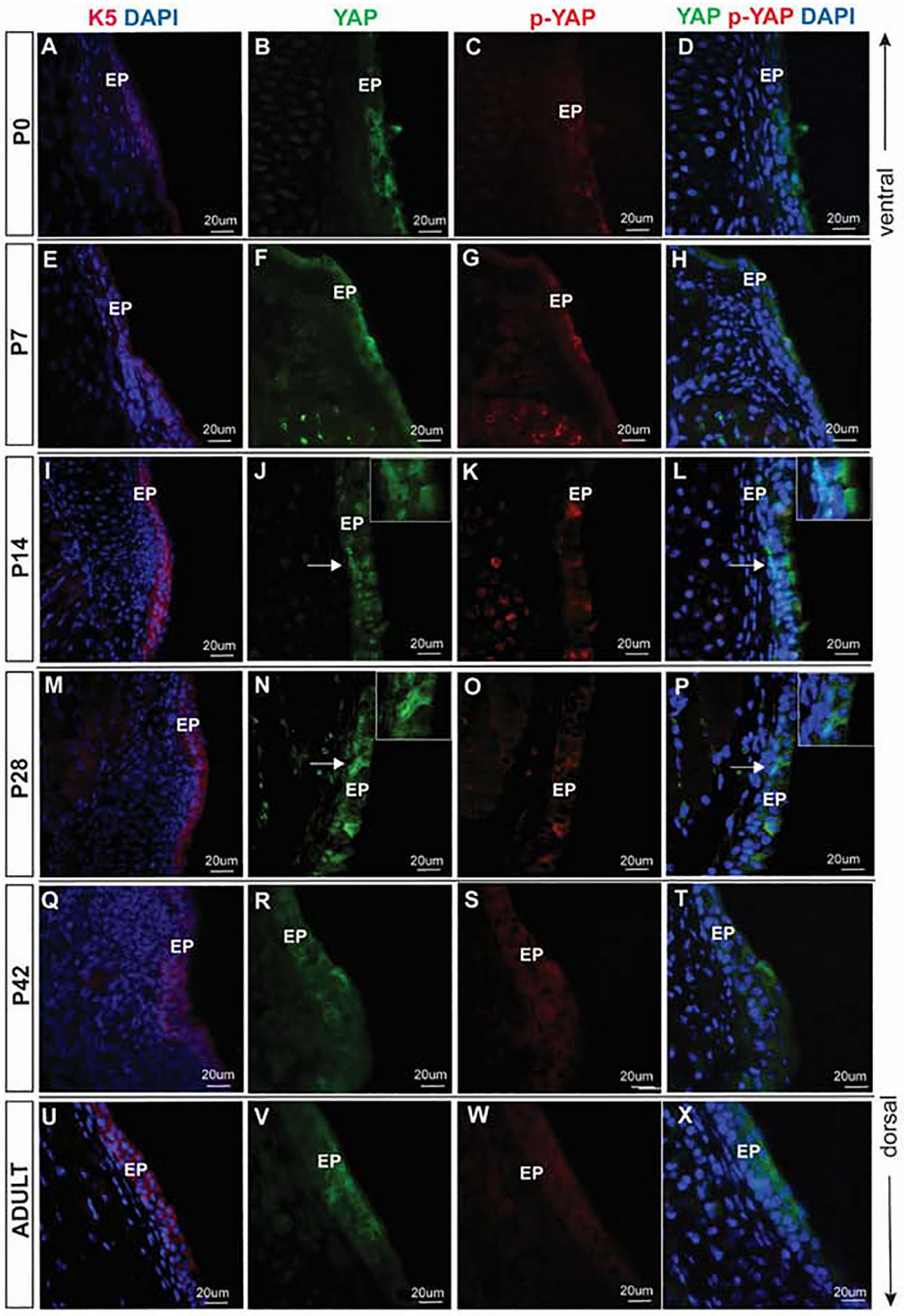

Figure 3: YAP expression during postnatal VF epithelial development.

(A-D) Transverse sections of mouse VF at P0. IF analysis of K5 (red) (A), total YAP (green) (B), p-YAP (red) (C) and double staining of YAP and p-YAP (yellow) (D). YAP is expressed mainly in the cytoplasm of K5 positive epithelial cells. (E-H) Transverse sections of mouse VF at P7. IF analysis of K5 (red) (E), total YAP (green) (F), p-YAP (red) (G) and double staining of YAP and p-YAP (yellow) (H). YAP continues to be expressed predominantly in the cytoplasm at this stage. (I-L) Transverse sections of mouse VF at P14. IF analysis of K5 (red) (I), total YAP (green) (J), p-YAP (red) (K) and double staining of YAP and p-YAP

(yellow) (L). At P14, a distinct cyto-nucleoplasmic shift is noted compared to the previous stage. YAP shifts from the cytoplasm to nucleus in some VF epithelial cells throughout the VF epithelium. White solid arrows in the panels of J, L denote nuclear YAP positive cells. These regions are magnified in the upper right corners of the same panels. (M-P) Transverse sections of mouse VF at P28. IF analysis of K5 (red) (M), total YAP (green) (N), p-YAP (red) (O) and double staining of YAP and p-YAP (yellow) (P). Similar to P14, at P28, a distinct cyto-nucleoplasmic shift is noted. In apical cells, YAP is highly phosphorylated and excluded from the nucleus, while basal cells exhibit prominent nuclear YAP localization. White solid arrows in the panels of N, P denote nuclear YAP positive cells. These regions are magnified in the upper right corners of the same panels. (Q-T) Transverse sections of mouse VF at P42. IF analysis of K5 (red) (Q), total YAP (green) (R), p-YAP (red) (S) and double staining of YAP and p-YAP (yellow) (T). YAP is again primarily localized to the cytoplasm in basal and apical cells. (U-X) Transverse sections of adult mouse VF. IF analysis of K5 (red) (U), total YAP (green) (V), p-YAP (red) (W) and double staining of YAP and p-YAP (yellow) (X). YAP is localized in the cytoplasm. A white dotted line at the panels of B, F, J, N, R, and V denotes basal versus apical cellular compartments. Primary antibodies are color-coded according to their secondary antibodies, and nuclei are counterstained with DAPI. All images are taken at 60X magnification; scale bar is 20 μm. Abbreviations: AC, apical cells; BC, basal cells; EP, epithelium.

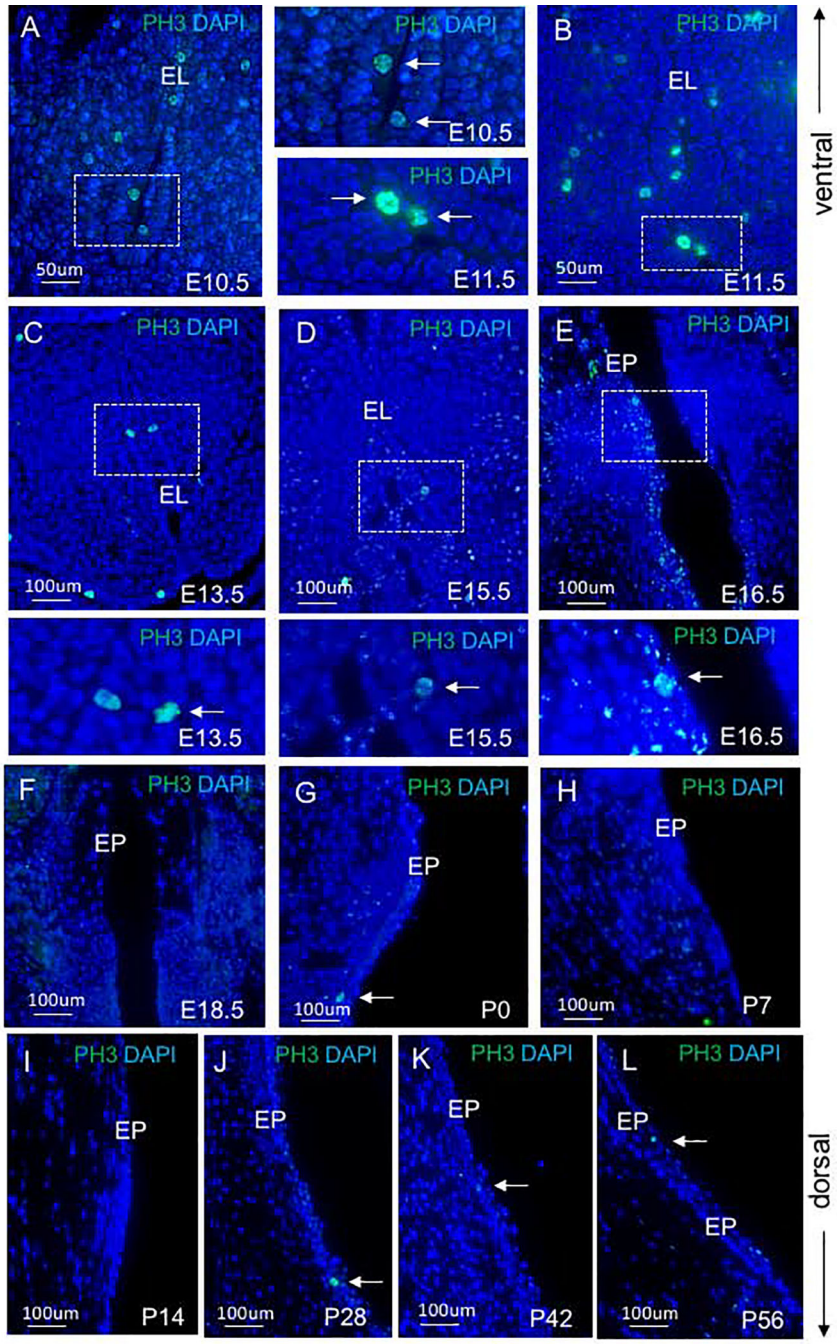

Figure 4: Cellular proliferation in VF epithelial cells across the developmental spectrum.

(A-L) Immunofluorescence analysis of PH3 (green) in transverse VF sections at E10.5 (A), E11.5 (B), E13.5 (C), E15.5 (D), E16.5 (E), E18.5 (F), P0 (G), P7 (H), P14 (I), P28 (J), P42 (K), P56 (L). The bracketed regions in the panels of A-E show PH3+ cells in detail. White solid arrows denote PH3 positive cells. For each developmental time-point (12 developmental stages in total), three larynges from three different individuals were dissected and analyzed (n=3; 36 WT larynges in total). Abbreviation: EL, epithelial lamina; EP, epithelium

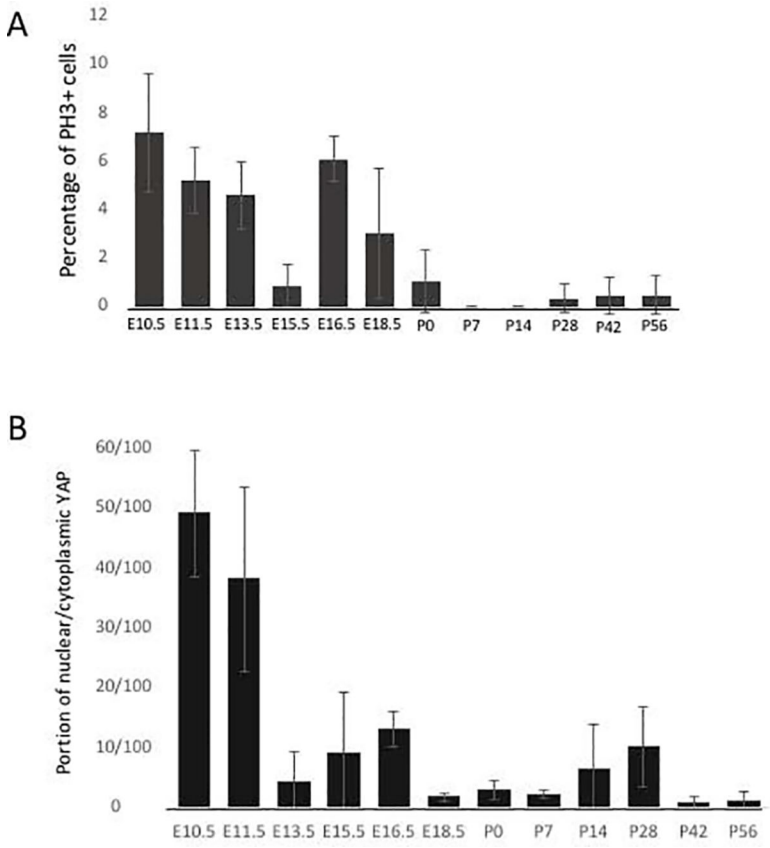

Figure 5: Quantitative assessment of cell proliferation and the portion of nuclear/cytoplasmic YAP positive VF epithelial cells throughout developmental stages.

(A) Quantitative assessment of PH3 positive cells in the VF epithelium throughout the VF developmental stages. (B) The portion of nuclear/cytoplasmic YAP positive cells in the VF epithelium throughout the developmental stages. For each developmental time-point (12 developmental stages in total), three larynges from three different individuals were dissected and analyzed (n=3; 36 WT larynges in total). A General Linear Model procedure with a one-way analysis of variance (ANOVA) determined $p < 0.0001$ for (A) PH3 and (B) nuclear/cytoplasmic YAP distribution across time points.

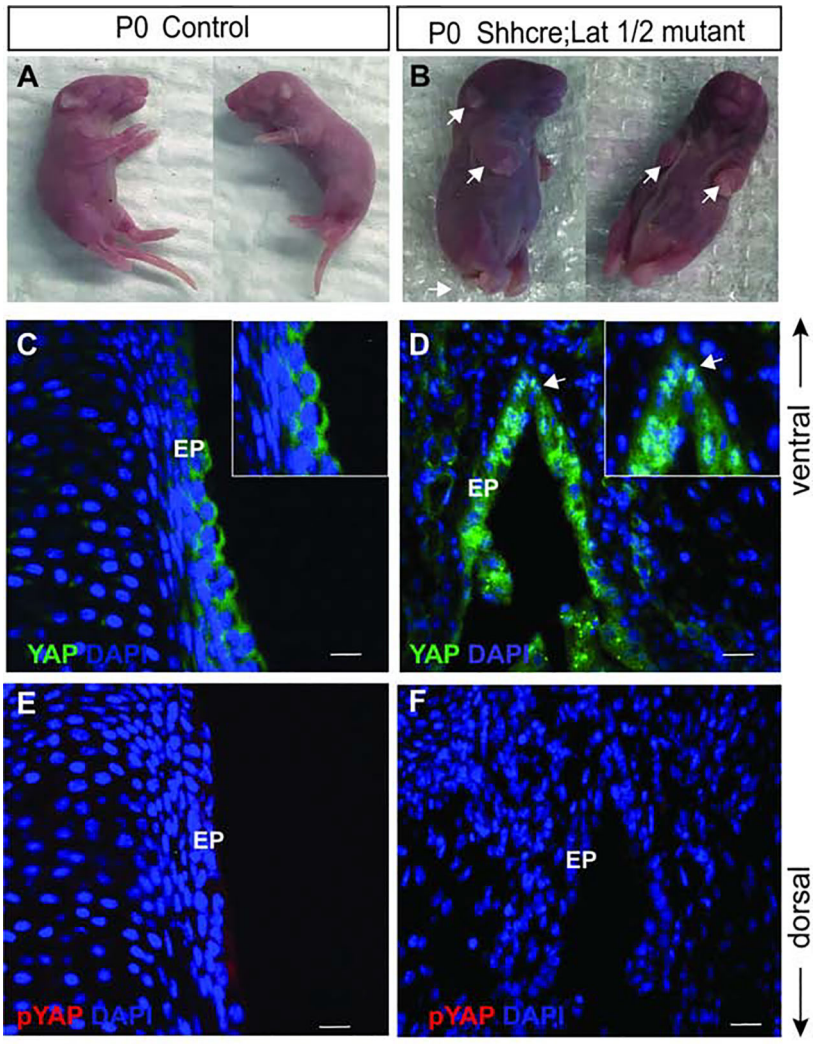

Figure 6: Conditional deletion of Lats1 and Lat2 result in developmental defects in Shhcre;Lats mutants.

(A-B) Whole embryo images of littermate controls at P0 (A) and Shhcre;Lats mutant animals at P0 showed limb, tail and skin defects (white arrows) (B). (C-D) Immunofluorescence detection of YAP (green) and DAPI (blue) in transverse section of VF of control (C) and Shhcre;Lats mutant (D). A white arrow in the panel of D indicates nuclear YAP in VF epithelium. Boxed magnified images in the upper right corners in the panel of C, D show YAP expression in the VF epithelium. (E, F) Immunofluorescence detection of p-YAP (red) in control (E) and Shhcre;Lats mutant (F) showing no p-YAP signal in mutant VF epithelium. Primary antibodies are color-coded according to their secondary antibodies, and nuclei are counterstained with DAPI (blue). IF images were taken at 60X magnification, scale is 20μm. Abbreviations: EP, epithelium.

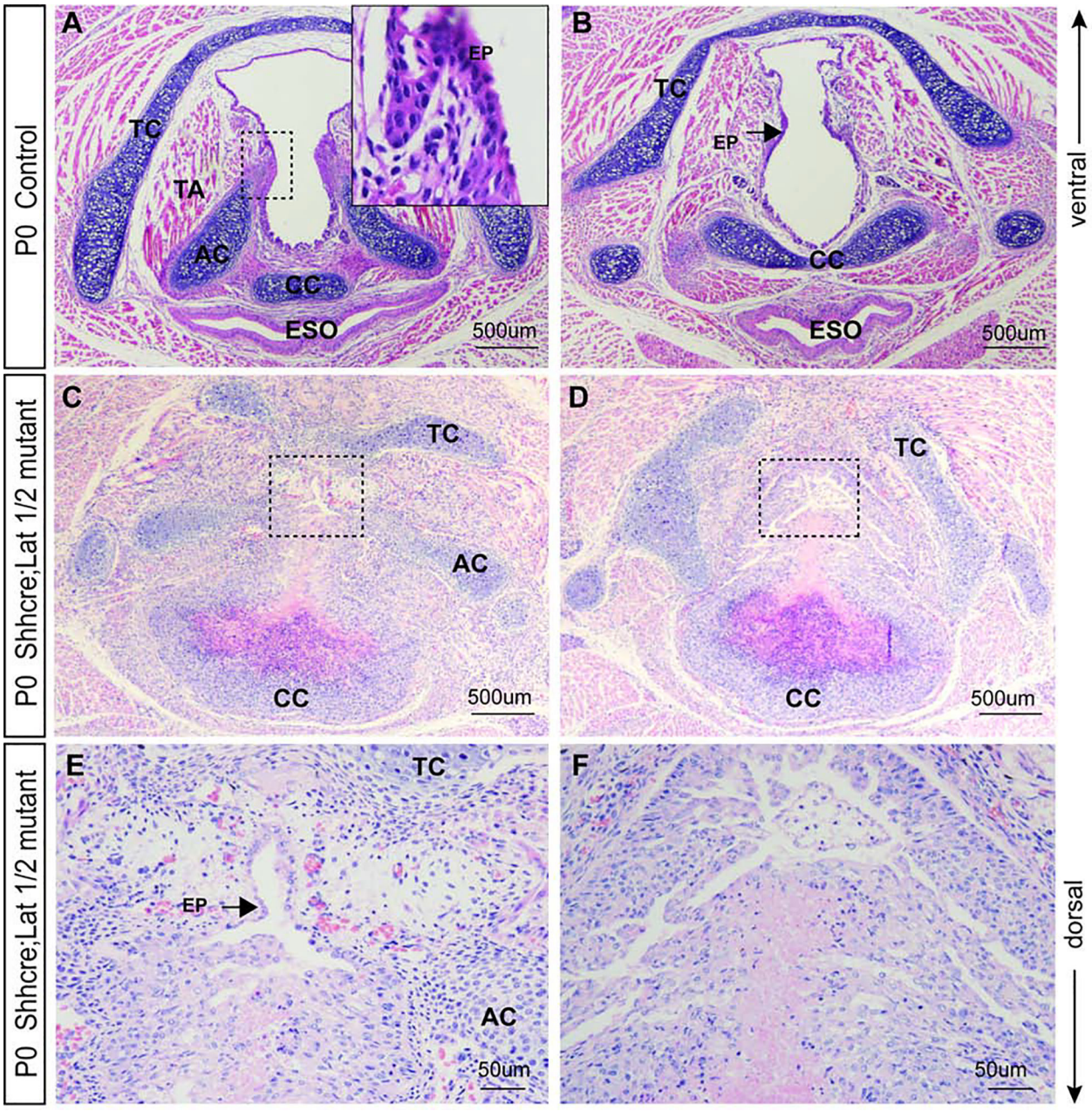

Figure 7: Nuclear YAP in the laryngopharynx significantly alters laryngeal morphology and causes severe morphogenetic defects in Shhcre;Lats mutants.

(A – B) Hematoxylin eosin staining in transverse sections demonstrating morphology in (A) glottal, and (B) subglottal regions of the VF in control embryos at P0. A bracketed region in the panel of A is magnified in the upper right corner and shows a two-layered VF epithelium. A black arrow in the panel of B denotes control VF epithelium. (C – D) Hemaoxylin&eosin staining in transverse sections demonstrating aberrant morphology in the (C) glottal and (D) subglottal region of the VF in Shhcre;Lats mutants at P0. (E - F) Bracketed regions in the panel of C, D are magnified in the panel of E, F respectively at 40X magnification. A solid black arrow in the panel of E denotes the unseparated, monolayered VF epithelium. The F panel shows the magnified view of VF subglottal section with aberrant

occlusion. Images were taken at 10X and 40Xmagnification. Scale bars are 500um and 50μm. Abbreviations: TC, thyroid cartilage; AC, arytenoid cartilage; CC, cricoid cartilage; ESO, esophagus; TA, thyroarytenoid muscle; PG, posterior glottis; EP, epithelium.

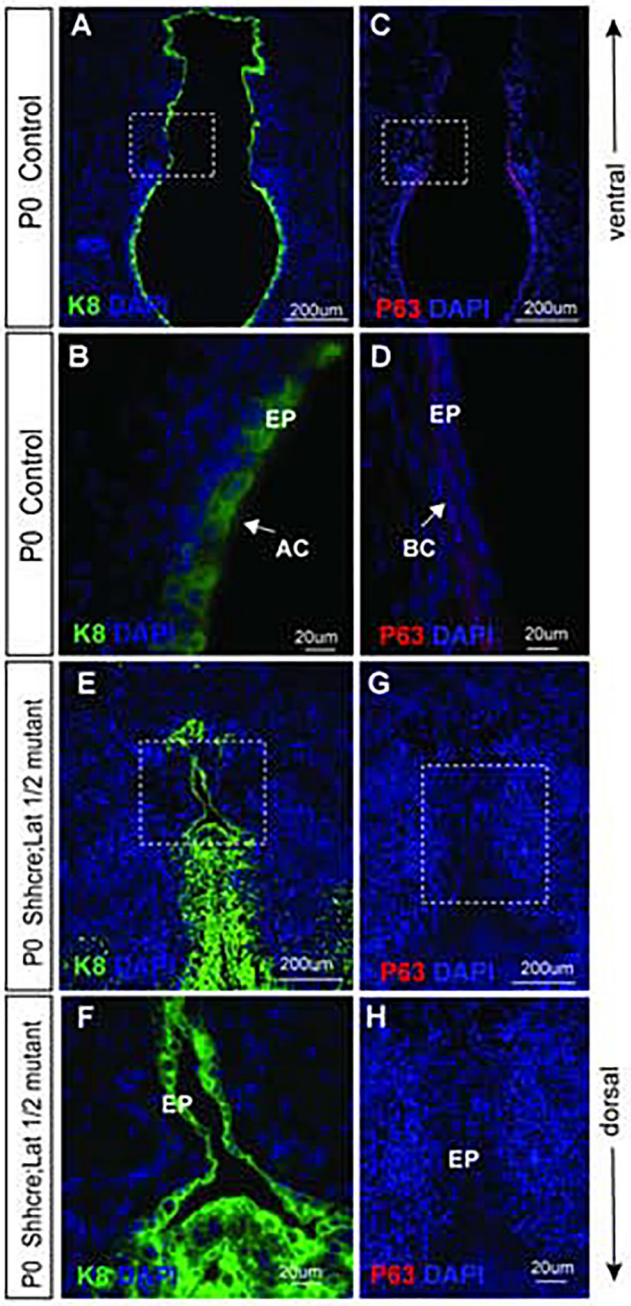

Figure 8: Inactivation of Lats1 and Lats2 results in the incomplete separation of the VF epithelium.

(A, B, and E, F) Immunofluorescence analysis of VF epithelial marker K8 (green) at P0 in transverse sections of the VF in controls (A, B) and Shhcre;Lats mutants (E,F). Bracketed regions in the panels of A and E are magnified in the B, F at 60X magnification respectively. Strong K8 (green) staining is seen in the VF epithelial layer in control and mutant VF epithelial cells. In Shhcre;Lats mutants K8 (green) staining of multilayered progenitors is seen in the not entirely separated VF epithelium. A white solid arrow in the panel of B denotes K8 positive VF apical cell layers. (C,D and G,H) Immunofluorescence analysis of

p63 (red) staining in transverse sections of control (C, D) and Shhcre;Lats mutant VF (G, H). Bracketed regions in the panels of C and G are magnified in the panels of D and H respectively at 60x magnification. A white arrow in the panel of D denotes p63 positive basal progenitors in control embryos. On the other hand, no p63+ progenitors are identified in the epithelial layer of the Shhcre;Lats mutant VFs at P0 (G,H). Primary antibodies are color-coded according to their secondary antibodies, and nuclei are counterstained with DAPI (blue). IF images were taken at 20X and 60X magnification. Scale bars of 200um and 20um were used in figure panels.

Abbreviation: EP, epithelium; BC, basal cells; ApC, apical cells.

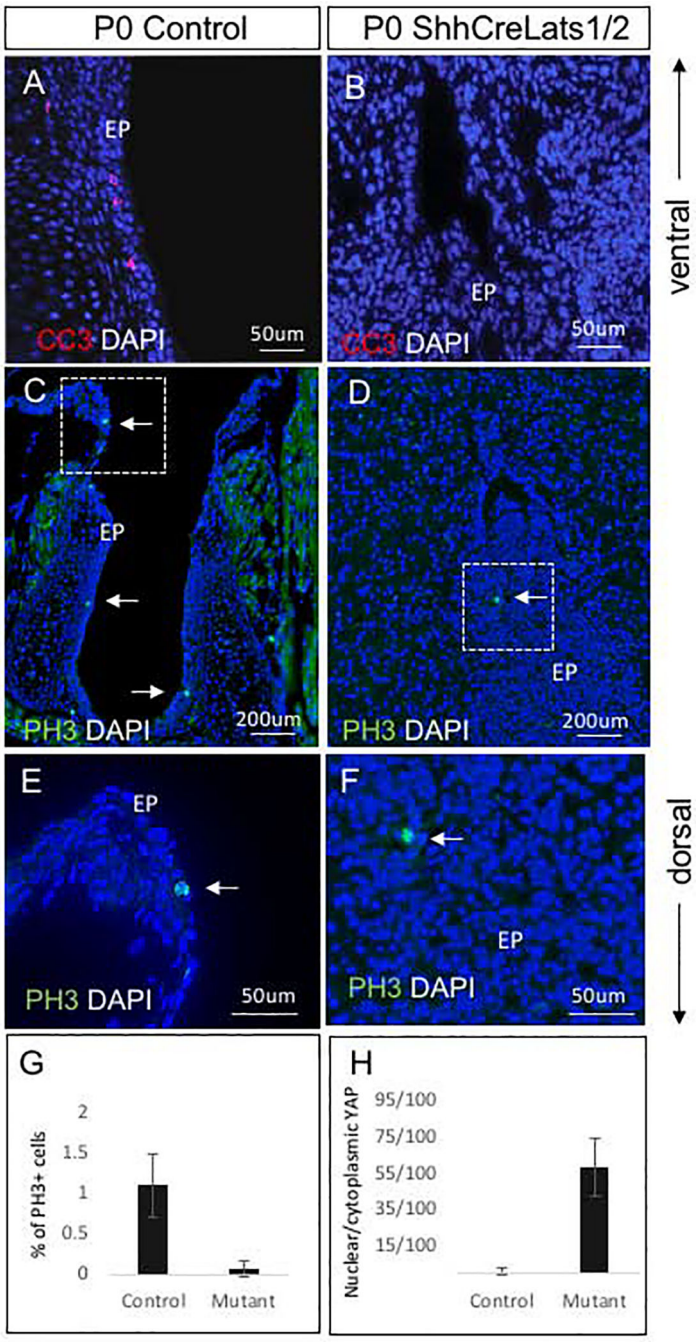

Figure 9: Apoptosis and cell proliferation analysis in Shhcre;Lats mutant VF at P0.

(A, B) Immunofluorescence detection of cleaved caspase 3 (red) and DAPI (blue) in littermate control VF (A) and Shhcre;Lats mutant VF (B). A transverse section of Shhcre;Lats mutant VF show no apoptotic cells (B). (C-F) Immunofluorescent detection of phospho-histone H3 (PH3) (green) and DAPI (blue) in the transverse sections of littermate control VF (C, E) and Shhcre;Lats mutants (D, F). Solid white arrows in the panels of C, D,E and F denote positive PH3 cells in green in control and mutant VF. Bracketed regions in the panels of C and D are magnified in the panels of E and F respectively. Considerably

decreased PH3 staining was detected in mutant VF epithelium. Primary antibodies are color-coded according to their secondary antibodies, and nuclei are counterstained with DAPI (blue). (G) Quantitative analysis of percentage of phosphohistone 3 (PH3) positive cells in the control versus mutant animals with a statistically significant difference measured between groups ($p = 0.002$) (H) Quantitative analysis of the proportion of nuclear/cytoplasmic YAP positive cells in controls and mutants with a statistically significant difference measured between groups ($p < 0.0001$). Abbreviations: EP, epithelium.

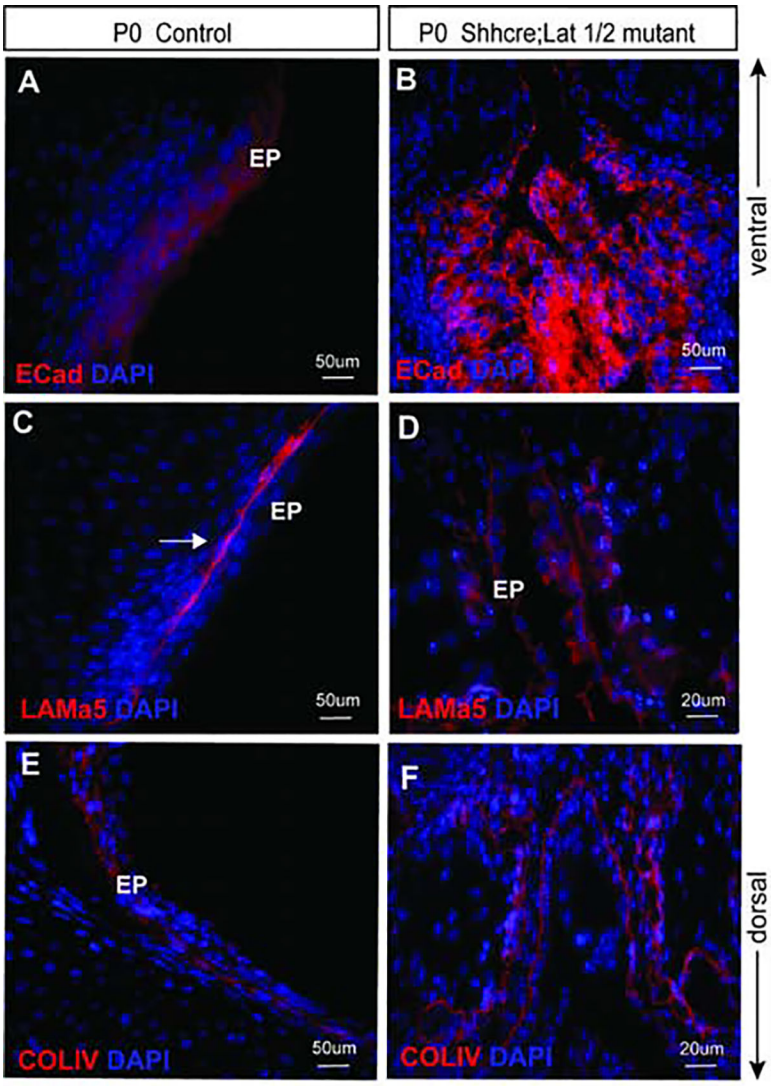

Figure 10: Shhcre;Lats mutant VF exhibit impaired cellular adhesion and structural changes in VF basement membrane components and integrity.

(A-F) Immunofluorescence analysis of E-Cadherin (red), Laminin α5 (in red), Collagen IV (in red) and DAPI (blue) in transverse sections of control (A, C and E) and Shhcre;Lats mutant VF (B, D and F). E-Cadherin is expressed in the VF epithelium in control embryos (A). In mutant VF, E-Cadherin expression is strong, altered and more localized to the basal surface of the epithelial progenitors (B). In control VF, Laminin α5 (red) is expressed strongly under layered epithelial cells (C). On the other hand, in Shhcre;Lats mutant VFs Laminin α5 is fragmented throughout the disrupted epithelium showing patchy and altered expression (D). Lastly, in control VF, Collagen IV (red) is expressed in the basement membrane, which is lined with epithelial cells luminally in the transverse section of control VF at P0 (E). In mutants, collagen IV is altered (F) and organized in two layers instead of a single monolayer. It appears fragmented and very similar to Laminin α5. Primary antibodies are color-coded according to their secondary antibodies, and nuclei are counterstained with DAPI (blue). IF images were taken at 20X, 40X and 60X magnification. Scale bars of

200um, 50um and 20um were used in figure panels. Abbreviations: AC, arytenoid cartilage; TC, thyroid cartilage; G, glottis; EP, epithelium.

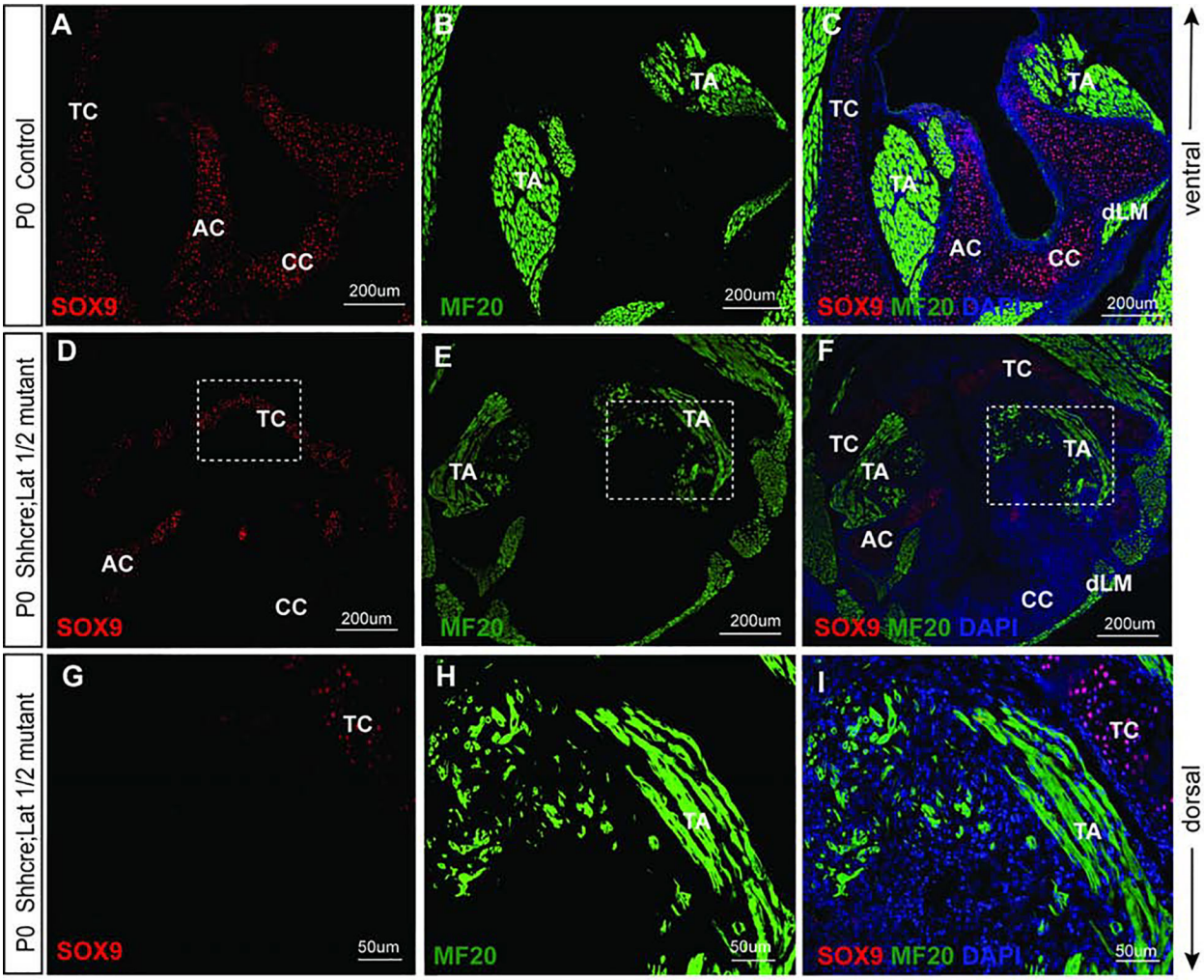

Figure 11: Nuclear YAP in epithelial cells causes mesenchymal defects as noted by distorted laryngeal cartilages and muscle development.

(A-I) Immunofluorescence detection of SOX9 (red), MF-20 (green) and DAPI (blue) in transverse sections of control (A-C) and Shhcre;Lats mutant VF (D-I) at P0. SOX9 (red) staining show SOX9 positive cells in developed laryngeal cartilages and MF-20 (green) staining shows completely developed laryngeal muscles in control VF (A-C). In the mutant larynx, VF show reduced SOX9 staining and defects in development of laryngeal cartilages (D-I) affecting the attachment of the laryngeal muscles. MF-20 staining shows altered structure and bulk of muscles fibers resulting in deformities in thyroarytenoid muscle and the dorsal laryngeal muscles. Primary antibodies are color-coded according to their secondary antibodies, and nuclei are counterstained with DAPI (blue). IF images were taken at 20X, and 40X magnification. Scale bars of 200um and 50um are used in the figure panels. Abbreviations: AC, arytenoid cartilage; CC, cricoid cartilage; TC, thyroid cartilage; EP, epithelium; TA, thyroarytenoid muscle; dLM, dorsal laryngeal muscles.

Table 1:

Primers used for genotyping

Transcript	Forward Primer (5’−3’)	Reverse Primer (5’−3’)	Product size
Shh CRE	GATGTGTTCCGTTACCAGCGA	ATGAACTTCAGGGTCAGCTTGC	400 bp
Lats1F	TTGTTGCTGGTGTTGTTTCC	ATGAATGAACCTGAGGCTGC	250 bp
Lats2F	AAAGCACAGGGCCTTTTA CAGCTTCCCCTG	CCACCCGCCACTGCACCTGAC CAGTATT	250 bp
Lats1D	AGGATGTAGTGAAGGCGTGTAAC	AGACCTCGTCGCACAGAATG	258 bp
Lats2D	CTATCGCTAGGCTGTTCCCAC	CTGAGCAACGACTCCAGGAAC	231 bp

Table 2:

Primary antibodies and dilutions

Primary Anitbody	Species	Dilution	Company	Catalogue No
Yap	Mouse	1:100	Santa Cruz Biotechnology, Dallas, Texas, USA	sc101199
Phospho-yap (Ser127)	Rabbit	1:500	Cell Signaling Technology	13008
Cytokeratin 8 (K8)	Mouse	1:100	Abcam Cambridge, UK	ab192467
Cytokeratin 5 (K5)	Rabbit	1:200	Abcam	ab193895
p63	Mouse	1:200	Santa Cruz Biotechnology,	sc8431
Phosphohistone H3 (H3)	Rabbit	1:1600	Cell Signaling Technology	9701
Cleaved caspase 3	Rabbit	1: 400	Cell Signaling Technology	9664
Laminin 5	Rabbit	1:100	Abcam	ab11575
E-cadherin Clone [24E10]	Rabbit	1:200	Cell Signaling Technology	3195
Collagen IV	Rabbit	1:100	Abcam	ab6586
SOX9	Rabbit	1:300	EMD Millipore, Billerica, MA, USA	ab5535

Table 3:

Secondary antibodies and dilutions

Secondary Antibody	Species	Dilution	Company	Catalogue No
Alexa Fluor 488	Goat anti mouse	1:1000	Invitrogen, Carlsbad, CA, USA	A11001
Alexa Fluor 594	Goat anti mouse	1:1000	Invitrogen	A11012
Cy-3 conjugated	Goat anti rabbit	1:200	Jackson ImmunoResearch; West Grove, PA, USA	125099